Field emission properties of nitrogen-doped diamond films

Cite as: Journal of Applied Physics **86**, 3973 (1999); https://doi.org/10.1063/1.371316
Submitted: 22 January 1999 • Accepted: 28 June 1999 • Published Online: 20 September 1999

A. T. Sowers, B. L. Ward, S. L. English, et al.

Field emission properties of nitrogen-doped diamond films

A. T. Sowers, B. L. Ward, S. L. English, and R. J. Nemanich[a)]
Department of Physics and Department of Materials Science and Engineering, North Carolina State University, Raleigh, North Carolina 27695-8202

(Received 22 January 1999; accepted for publication 28 June 1999)

This study explores the field emission properties of nitrogen-doped diamond grown by microwave plasma chemical vapor deposition. Over 70 nitrogen-doped diamond samples were grown on silicon and molybdenum under varying process conditions. Under certain conditions, films can be grown which exhibit photoluminescence bands at 1.945 and 2.154 eV that are attributed to single substitutional nitrogen. Photoelectron emission microscopy with UV free electron laser excitation indicated a 0 or negative electron affinity. Field emission characteristics were measured in an ultrahigh vacuum with a variable distance anode technique. For samples grown with gas phase [N]/[C] ratios less than 10, damage from microarcs occurred during the field emission measurements. Samples grown at higher [N]/[C] content could be measured prior to an arcing event. Contrary to other reports on nitrogen-doped diamond, these measurements indicate relatively high threshold fields (>100 V/μm) for electron emission. We suggest that the nitrogen in these films is compensated by defects. A defect-enhanced electron emission model from these films is discussed. [S0021-8979(99)05719-9]

I. INTRODUCTION

Diamond has been considered as a material of choice for next-generation cold cathode materials. The strong sp^3 bonding character in diamond leads to a material with unique mechanical, chemical, and electrical properties that are particularly suitable for the harsh environments found in cold cathode applications. In addition, properly prepared diamond surfaces have been shown to exhibit a negative electron affinity (NEA).[1–5] A NEA occurs when the vacuum level lies below the conduction band minimum at the semiconductor/vacuum interface. The presence of a NEA for a semiconductor means that electrons in the conduction band can be freely emitted into vacuum without a barrier. This principle has motivated extensive research in the development of diamond based cold cathodes for vacuum microelectronics including flat panel displays and high power microwave amplifiers.

While the ideal cathode material would exhibit a NEA as noted above, other properties are equally if not more important. In the most basic sense, field emission from a semiconductor involves the supply of electrons to the material, transport through the bulk, and finally emission at the surface. To achieve these properties, *n*-type semiconducting characteristics are desired. Highly doped *n*-type material will allow low resistance contacts and provide electrons for transport through the material. To date, efforts have been limited by the lack of a reliable shallow *n*-type dopant for diamond.

Nitrogen has a high solubility in diamond and is found in both natural and synthetic diamonds. In synthetic high pressure, high temperature (HPHT) type-Ib single crystal diamond, nitrogen is present in primarily single substitutional form with a relatively deep donor level located $\sim$1.7 eV below the conduction band minimum.[6,7] In 1996 Geis *et al.* reported an enhancement of field emission properties of single crystal nitrogen-doped diamond.[8] In that study, nickel was deposited as the back contact on nitrogen-doped crystals. It was reported that this metallization created a Schottky contact forming a narrow depletion layer. In this model the applied voltage drops primarily across the depletion layer at the nickel/diamond interface. Electrons tunnel into the diamond conduction band through the narrow depletion region and are emitted into vacuum at the NEA surface. A simplified band diagram illustrating this emission mechanism is shown in Fig. 1. More recently, Geis *et al.* have reported another electron emission mechanism from type-Ib single crystal diamond.[9] This model is a surface-emission model in which electrons tunnel from the metal back contact into surface states at the interface of nitrogen-doped diamond and vacuum.

Okano *et al.* have reported threshold fields less than 1 V/μm for nitrogen-doped diamond films grown by hot-filament chemical vapor deposition (CVD) using urea as a nitrogen doping source.[10] Using Rutherford backscattering, the nitrogen content in the deposited films was found to be $\sim 10^{20}\,\mathrm{cm}^{-3}$. However, no evidence of single substitutional nitrogen doping was presented. It is possible that the nitrogen incorporated into these films is segregated at the grain boundaries or in nitrogen aggregates commonly observed in natural diamond crystals. These urea-doped diamond samples have also been studied by Matsuda and coworkers.[11] Using x-ray photoelectron spectroscopy (XPS), significant amounts of oxygen and tungsten incorporation were observed (>20 and ~ 3 at. %, respectively). It is not evident what effect these additional impurities may have in the field emission process. In these studies the threshold fields required for electron emission were higher (from 8.0 to 4.5 V/μm) than reported by Okano *et al.* and arcing was observed during some measurements. Despite these pub-

a)Electronic mail: Robert_Nemanich@ncsu.edu

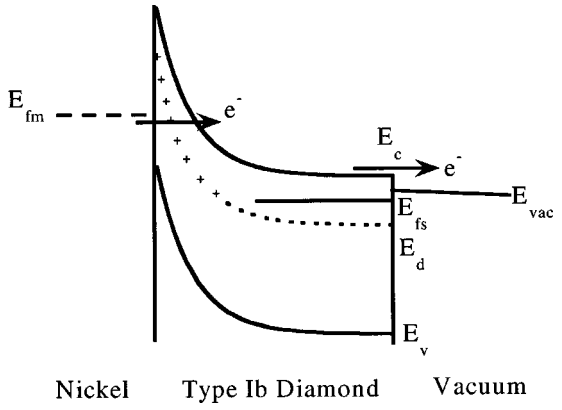

FIG. 1. Energy band diagram illustrating the field emission mechanism proposed by Geis *et al.* (Refs. 8 and 9). In this model, a depletion layer is formed when an electric field is applied across the diamond. Electrons tunnel from the metal contact into the conduction band of the diamond, and are emitted at the NEA surface. This figure is shown for a large applied bias.

lished reports, the mechanisms governing field emission from nitrogen-doped diamond have not yet been determined.

This study explores the field emission properties of nitrogen-doped diamond grown by microwave plasma CVD. The reports from Geis *et al.* discussed above indicate that electrons may be injected into the diamond conduction band through the substrate/diamond interface. As a result, the role of this interface was studied by depositing nitrogen-doped diamond on both silicon and molybdenum substrates using various nucleation techniques. Evidence of single substitutional nitrogen incorporation was confirmed by photoluminescence measurements. The electron emission properties of these diamond films were examined with field emission characterization, and photoemission electron microscopy (PEEM). In contrast to the reports described above, the results of this study indicate that nitrogen doping produces diamond films with average threshold fields often exceeding 100 V/μm. In addition, arcing is frequently observed during field emission characterization causing extensive physical damage to the sample. A mechanism describing field emission from these nitrogen-doped diamond films is also presented.

II. EXPERIMENT

Nitrogen-doped diamond films were deposited in a commercially available ASTeX HPMS stainless steel microwave (2.45 GHz) plasma CVD deposition chamber. *In situ* growth rate and film thickness information was monitored using laser reflectance interferometry (LRI). For this technique, a HeNe laser ($\lambda = 632.8$ nm) was directed onto the substrate at normal incidence. During growth, interference between reflections from the vacuum/diamond and diamond/substrate interfaces causes the reflected light to oscillate as a function of time. By recording the reflected intensity with a silicon photodiode, the thickness of the film can be measured by counting the number of interference ''fringes.'' Details of using the LRI technique to monitor diamond growth may be found elsewhere.[12,13]

The conventional gas mixtures of hydrogen and methane were used as the growth precursors. Two sources of nitrogen were used depending on the desired nitrogen concentration in the process gas. For low nitrogen process concentrations a mixture of nitrogen (2.11%) diluted in hydrogen was used. For high nitrogen concentrations zero-grade nitrogen (99.998% minimum purity) was directly admitted to the process gas. With these two sources, nitrogen could be added as an impurity to the process gas with gas phase atomic nitrogen to carbon ratios ([N]/[C]) from 0 to 80.

Polycrystalline diamond films containing nitrogen were deposited on 25-mm-diam *n*-type (1 Ω-cm) (100) silicon or mirror polished molybdenum substrates. Either diamond grit polishing or biased enhanced nucleation (BEN) was employed to enhance nucleation. The diamond scratched substrates were hand polished for 10 min using 1–2 μm diamond powder applied to a nylon polishing cloth. Before loading into the chamber, the scratched substrates were cleaned ultrasonically in acetone and methanol to remove residual diamond powder. For depositions using BEN, the substrates were loaded into the diamond growth chamber without any pretreatment. Before BEN, the untreated substrates were exposed to a hydrogen plasma in the diamond growth chamber for 10 min. Nucleation densities of 10^9 cm^{-2} or greater have been achieved with these nucleation techniques. This is critical for the formation of continuous films used in this study.

For both the scratched and BEN samples, diamond nucleation was achieved at ~760 °C surface temperature, 600 W microwave power, 20 Torr chamber pressure, and a flow rate of 400 sccm using process gases consisting of 2 vol % methane in hydrogen. The samples employing BEN were biased −200 V during the nucleation phase of growth. Nucleation time was determined by monitoring the reflected LRI beam for an initial drop in reflectivity indicating sufficient nucleation.[12] For both techniques, the nucleation time was ~21 min for most samples. Following the nucleation step, the substrate temperature, microwave power, chamber pressure, and process gases were changed to the growth conditions.

Nitrogen-doped diamond films were grown at substrate temperatures from 800 to 900 °C, 1300 W microwave power, and 50 Torr chamber pressure. The growth process gases consisted of 0.5 vol % methane and 0–12 vol % nitrogen in hydrogen at a total flow rate of 500 sccm. All samples were grown ~1 μm thick by monitoring the LRI oscillations.

After growth, room temperature micro-Raman and photoluminescence spectra were recorded with an ISA U-1000 scanning double monochromator using the 514.5 nm line of an argon ion laser as the excitation source. The laser beam was focused on the samples to a spot size of ~3 μm diameter using an Olympus BH-2 microscope. Low temperature photoluminescence (PL) measurements were also measured using the same monochromator in a macroconfiguration. For these measurements the sample was mounted to a Janis CCS-350 closed cycle helium refrigerator system. In the macroconfiguration the laser was focused to a line of approximately 100 μm × 2 mm.

After optical characterization, the nitrogen-doped diamond samples were mounted on molybdenum sample holders and transferred into the loadlock of a multichambered ultrahigh vacuum (UHV) system. This UHV system is equipped with a ~14-m-long linear transfer mechanism which interconnects 10 different analysis and surface processing chambers. The chambers used in this study include hydrogen plasma processing, XPS, Auger electron spectroscopy (AES), and variable distance anode field emission. The ultrahigh vacuum (UHV) system has been described in more detail elsewhere.[14]

Before field emission measurements were obtained, the diamond samples were typically exposed to a remote hydrogen plasma to remove adsorbed species and hydrogen terminate the surface. The hydrogen plasma clean consisted of a 1 min exposure to a 50 W rf plasma discharge at ~25 mTorr. The sample temperature was held at 500 °C during the plasma treatment. This atomic hydrogen exposure has been shown to induce a NEA on several different diamond surface orientations.[3] The nitrogen-doped diamond films were also examined with XPS and AES to identify the chemical composition at the sample surface. XPS analysis was performed using Al $K\alpha$ ($h\nu = 1486.6$ eV) radiation and a VG CLAM II electron analyzer. AES spectra were obtained using a beam voltage of 3 keV and an emission current of ~1 mA using a Perkin–Elmer cylindrical mirror analyzer (CMA).

The field emission measurements employed a variable distance anode, which was stepped toward the surface and current–voltage ($I-V$) measurements were obtained at various anode-to-sample distances. The measurements were conducted in a UHV environment with pressures typically $<5\times10^{-9}$ Torr. A cylinder of molybdenum (3 or 1 mm in diameter) was chosen as the anode for these measurements. The end of the cylinder was either polished flat or polished to a very high radius of curvature (typically >5 mm) to minimize edge effects. The anode is mounted on a stage that is coupled to a UHV stepper motor. The stepper motor controls the distance between the anode and the sample such that one step of the motor results in a translation of the anode by 55 nm. The $I-V$ measurements are acquired with a computer controlled Keithley 237 Source-Measure Unit (SMU). The SMU has the ability to simultaneously supply a voltage and measure a current. A current limiting circuit is also included within the SMU so that no voltage is applied that causes the current to exceed 1×10^{-8} A. Although the anodes used in this study were rounded, it is assumed that the electric field between the anode and the sample surface can be modeled by the parallel plate geometry. This assumption is valid since the radius of curvature is very large in comparison to the distance, d, between the anode and the sample (cathode). In the parallel plate geometry the electric field is given by $E = V/d$, where V is the applied voltage between the anode and the cathode. As a result, if a particular electric field, $E_{\text{threshold}}$, is required for field emission from a cathode surface, then the required applied voltage is given by $V_{\text{threshold}} = E_{\text{threshold}}\times d$. From this expression, it is evident that the voltage required for emission is linearly dependent upon d, the distance between the anode and the sample (cathode).

For any given field emission measurement, a family of $I-V$ curves is recorded with each curve corresponding to a different anode-to-sample spacing. Initially, the anode is positioned at some unknown distance above the sample. The stepper motor count is recorded and an $I-V$ curve is collected. Next, the anode is moved closer to the sample by a known distance and the cycle is repeated until at least 5–10 curves are collected. As expected, the $I-V$ curves shift to lower voltage values with decreasing anode to cathode distance.

Due to the exponential nature of the field emission $I-V$ curves, the ''turn-on'' voltage or threshold voltage must be defined in terms of a specific current value. In this study, the voltage that results in a current value of 0.5 nA was chosen to represent the threshold voltage for electron emission. In order to prevent microarcs for these nitrogen-doped diamond films, it was necessary to limit the current to 0.5 nA and less. Each threshold voltage is then plotted versus distance relative to the first $I-V$ curve, and as expected, the resulting graph was linear. Upon fitting the data to a straight line, the slope represents the average field for the threshold current emission. This method for determining the average field does not rely upon the absolute anode to sample spacing, but rather an accurate measurement of the change in distance of the anode with respect to the sample. In addition, this technique has the advantage that the anode is never in contact with the sample.

The electron emission characteristics of these samples were imaged using PEEM in a high-resolution system from Elmitec. In PEEM measurements, photoelectrons are excited by ultraviolet radiation. These photoelectrons are accelerated into an electromagnetic immersion lens, which has a lateral resolution of 10 nm. In this lens, 20 kV is applied over a distance of 2 mm resulting in an average field of 10 V/μm at the sample surface. Once the photoemitted electrons accelerate through this objective lens, they are magnified and focused by a series of lenses onto a microchannel plate and phosphor screen. A charge coupled device (CCD) camera records the image. The spontaneous emission from a free electron laser system was used as the ultraviolet light source. The light was obtained from the OK-4 UV free electron laser (FEL) at the Duke University Free Electron Laser Laboratory. The PEEM technique and applications have been described in greater detail elsewhere.[15,16]

III. RESULTS

The goal of this work is to investigate the role of nitrogen doping on the field emission properties of diamond. Previous field emission results from intrinsic and *p*-type diamond films have indicated lower threshold fields for samples with higher defect densities as measured by Raman scattering spectroscopy.[17] As a result, our efforts were to produce high quality nitrogen-doped films, and not to deliberately deposit highly defective films. For this reason, diamond films were grown with 0.5 vol% methane. Undoped diamond films grown under these conditions are known to result in films of high quality. Despite this objective, as will be seen

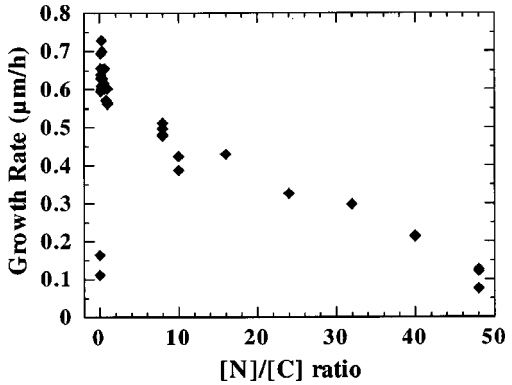

FIG. 2. Growth rates from several nitrogen-doped diamond films with [N]/[C] ratios from 0 to 48. Growth rate information was obtained by monitoring the LRI oscillations during growth.

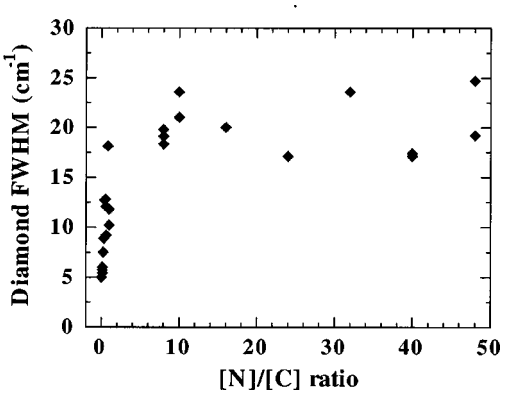

FIG. 4. The FWHM of the diamond Raman line of the spectra in Fig. 3 as a function of [N]/[C] in the process gas.

below, the addition of nitrogen to the process gas changes the growth chemistry and results in lower film quality.

In this study over 70 nitrogen-doped films were grown with gas phase [N]/[C] ratios from 0 to 48. It was observed that the addition of low amounts of nitrogen initially enhances the growth rate by a factor of ~4.5. However, for [N]/[C] ratios greater than 0.3 the growth rate decreases with increasing nitrogen addition. Ultimately for [N]/[C] ratios greater than 48, no deposition is observed, and the silicon substrates are visibly roughened. The growth rates for the nitrogen-doped diamond films grown in this study are shown in Fig. 2.

The Raman spectra for nitrogen-doped diamond films grown on silicon at ~900 °C with various gas phase [N]/[C] ratios are shown in Fig. 3. For reference, the spectra for a diamond film grown without nitrogen is also included in the figure. As stated earlier, the addition of low quantities of nitrogen leads to a decrease in diamond film quality. In addition to the diamond Raman line at 1332 cm^{-1}, peaks associated with graphite at ~1350 and ~1580 cm^{-1} are present in the spectra and become more prominent with increasing nitrogen content in the process gas. Other peaks from microcrystalline diamond and sp^2 bonding in diamond are also visible at 1140 and ~1500 cm^{-1}, respectively. At high nitrogen concentrations, peaks (at 1190 and 1550 cm^{-1}) possibly attributed to N–C complexes are evident in the spectra, however, more work needs to be performed to determine their identity.[18] In Fig. 4, the full width at half maximum (FWHM) of the diamond Raman line for several diamond films is plotted as a function of [N]/[C]. We can conclude from Figs. 3 and 4 that as the nitrogen content in the process gas increases, the amount of nondiamond carbon in the deposited film increases and the defect density within the diamond crystallites also increases.

For gas phase [N]/[C] ratios from 0.1 to 1.0 and growth temperatures of ~900 °C, nitrogen-doped diamond films can be deposited which exhibit photoluminescence (PL) bands attributed to nitrogen+vacancy optical centers. These bands are a characteristic of single substitutional nitrogen doping in diamond seen in type-Ib HTHP synthetic diamond. The room temperature PL spectra for several nitrogen-doped diamond samples exhibiting these luminescence features are shown in Fig. 5. The zero-phonon lines (ZPL) for these nitrogen-related bands are found at 1.945 and 2.154 eV. The intensity of these nitrogen related centers decreases with increasing nitrogen process content. A possible explanation for this trend is the quenching of the luminescence in the presence of a high concentration of defects. This is consistent with the Raman spectra shown in Fig. 3.

All of the nitrogen containing films which were deposited on Si substrates showed a relatively strong 1.680 eV band. The 1.680 eV band has been attributed to silicon in-

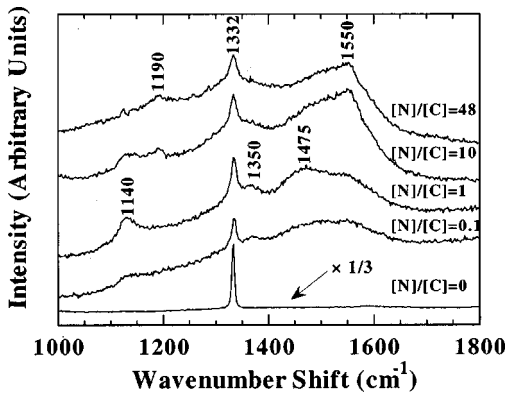

FIG. 3. Raman scattering spectra for several nitrogen-doped films deposited on silicon at ~900 °C with [N]/[C] ratios from 0 to 48. The addition of nitrogen to the process gas increases nondiamond bonding in the films.

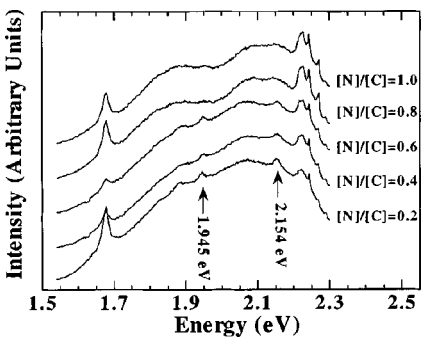

FIG. 5. Photoluminescence spectra recorded at room temperature for nitrogen-doped diamond films grown on silicon with gas phase [N]/[C] from 0.2 to 1.0. The presence of the luminescence bands at 1.945 and 2.154 eV indicate single substitutional nitrogen incorporation.

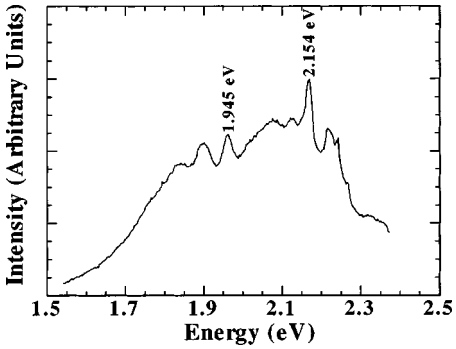

FIG. 6. Low temperature PL spectra recorded at 10 K for a nitrogen-doped film grown on molybdenum. Low temperatures enhance the nitrogen related luminescence because electron lattice interactions are reduced.

corporation in diamond films.[18] One possible explanation is that nitrogen containing species in the plasma increases the silicon etch rate during growth, causing increased silicon incorporation. It is difficult to account for the observed trend in the 1.680 eV signal other than noting that it could be related to changes in the film microstructure. A possible unwanted effect of silicon incorporation could be the compensation of the single substitutional nitrogen donors. For this reason, molybdenum was also chosen as a substrate material. Nitrogen-doped films grown on molybdenum substrates exhibit no silicon related luminescence.

At higher temperatures (i.e., room temperature), there is significant electron–lattice interaction. The effect of this interaction is to reduce the ZPL intensity of the nitrogen related luminescence while increasing the vibronic sideband intensity. Conversely at low temperatures, there are less phonons available in the material to interact with the optical center transitions. For this reason, photoluminescence measurements were also recorded at low temperatures for the nitrogen-doped films in this study. PL spectra recorded at 10 K for a nitrogen-doped diamond film grown on molybdenum are shown in Fig. 6. The effect of this electron–lattice interaction is easily distinguished. The presence of these PL bands for these films indicates that nitrogen is being incorporated into the diamond providing a donor level located ~1.7 eV below the conduction band minimum.

Figure 7 shows scanning electron microscopy (SEM) micrographs of the surface morphologies of several diamond films examined in this study. Without nitrogen addition, the diamond film morphology typifies high quality diamond growth with well faceted grains. However as seen in the figure, the addition of nitrogen degrades this faceting and ultimately produces extremely fine-grained diamond films at the highest nitrogen process gas concentrations.

After H-plasma cleaning, nitrogen-doped samples were analyzed with XPS and AES to identify the chemical composition of the films. Despite evidence of nitrogen incorporation in the PL spectra, only carbon was observed in XPS and AES. For reference, the minimum detection limits of XPS and AES are ~0.1 at % and ~1.0%, respectively. It should be stressed at this point that neither oxygen nor metallic impurities were detected.

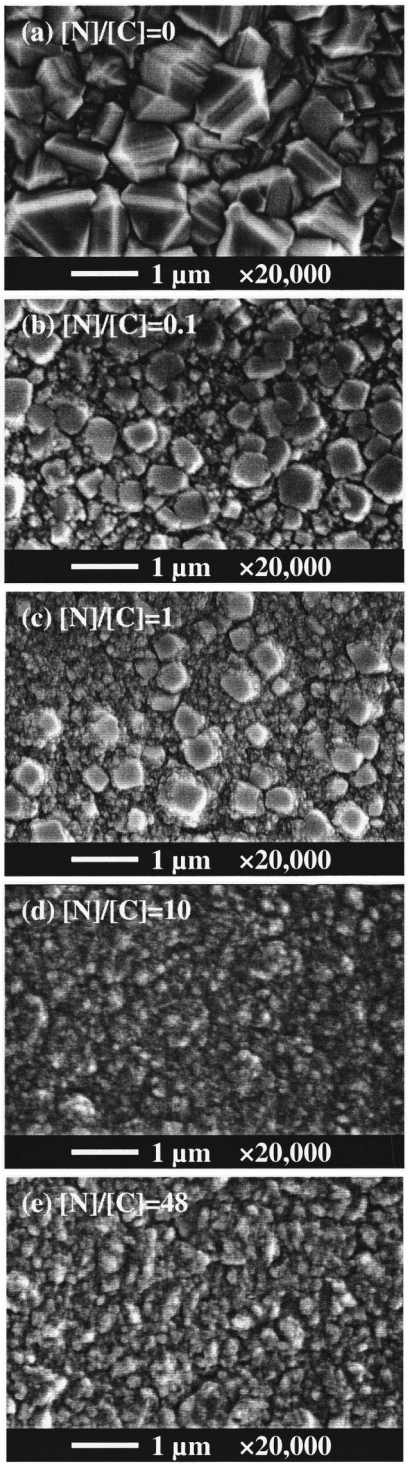

FIG. 7. Scanning electron micrographs of the surfaces of several nitrogen-doped films examined in this study. For reference, an undoped diamond film is also shown.

Initially, the distance variable anode technique was used to characterize the field emission properties of the nitrogen-doped films using procedures developed for other wide band gap materials. Several experiments were performed to evaluate the effect of nitrogen doping upon the threshold field required for electron field emission. However, these measurements produced widely varying and often irreproducible results. In fact, threshold fields for emission often varied be-

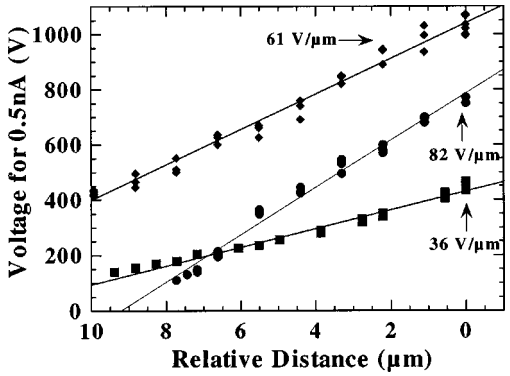

FIG. 8. Threshold voltage as a function of distance for a nitrogen-doped film in which arcing occurred during computer controlled auto approach. The slope of each line represents the threshold field required for 0.5 nA of emission current. Each line represents a series of $I-V$ measurements, which were taken at three different places near the center of the film.

tween 9 and 80 V/μm for different regions on the same sample. Three field emission measurements on a nitrogen-doped film illustrating this instability are shown in Fig. 8.

It was only after the diamond surfaces were examined after field emission that the reason for this unstable behavior was evident. Micrographs of these surfaces revealed arc-damaged sites similar to features reported by Gröning *et al.*[19] It was established that the damage occurred during a computer controlled auto-approach sequence. Consequently for later measurements, a manual approach technique was used to place the anode appropriately above the sample surface.

Despite the refinements in the field emission measurements, microarcing was still observed for all films with [N]/[C] ratios less than 10. It should be pointed out that this behavior was observed regardless of the nucleation technique or substrate material. For these films, microarcing occurred during the first $I-V$ measurement just after the current rose above the baseline noise level ($\pm 2\times 10^{-11}$ A) in the test system. Microarcs are detected by monitoring the $I-V$ curves for large discontinuous jumps in the measured current. Figure 9 shows an $I-V$ curve illustrating an arcing event. If field emission measurements are continued after microarcing, average threshold fields for electron emission again range from 9 to 80 V/μm depending upon the magnitude of the damage to the film and substrate. It is evident that measurements from arc-damaged surfaces are not indicative of the nitrogen-doped diamond film properties, but rather from the damaged material and sharp protrusions from the surface produced by the microarc.

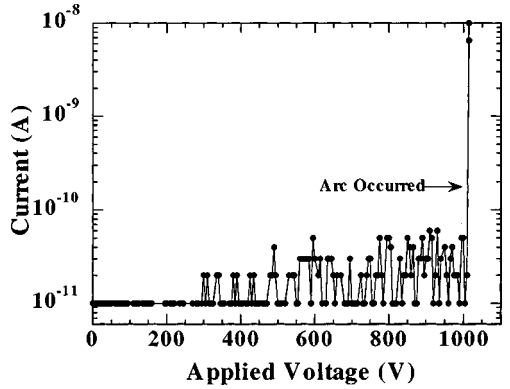

FIG. 9. Current–voltage curve during a field emission measurement in which an arcing event occurred. Note the discontinuous jump in the current at the end of the curve.

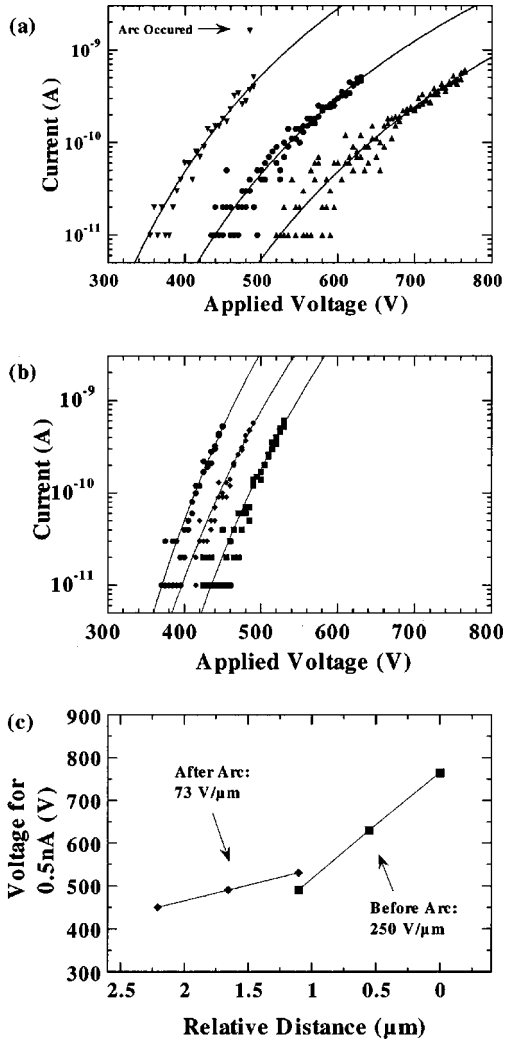

FIG. 10. Field emission measurements from a nitrogen-doped film grown on molybdenum with [N]/[C]=10 in which an arc occurred during the measurements [the solid lines represent fits using the Fowler–Nordheim relation: $I=C_1V^2\exp(-C_2/V)$]. Current–voltage measurements are taken at several anode-to-sample distances and are shown in (a) and (b). $I-V$ measurements recorded before the arcing event are shown in (a). During the third $I-V$ measurement an arc occurred. The $I-V$ measurements taken after the arcing event are shown in (b). It is evident that the shape and the signal-to-noise ratio changes after the arc. The threshold field analysis for this data set is shown in (c). The threshold fields required to obtain 0.5 nA of current before and after the arc are 250 and 73 V/μm, respectively.

For nitrogen-doped films with [N]/[C]$\geqslant$10, field emission could be observed without being preceded by an arcing event. Usually for these samples, approximately five $I-V$ curves could be collected before an arcing event occurred. Analysis of data collected before arcing, indicate that the average threshold fields required for emission are 100–300 V/μm. After arcing, the threshold fields are again reduced to 9–80 V/μm. Figure 10 shows the field emission data collected from a sample grown with [N]/[C]=10. During this experiment an arc occurred at the end of the third $I-V$ mea-

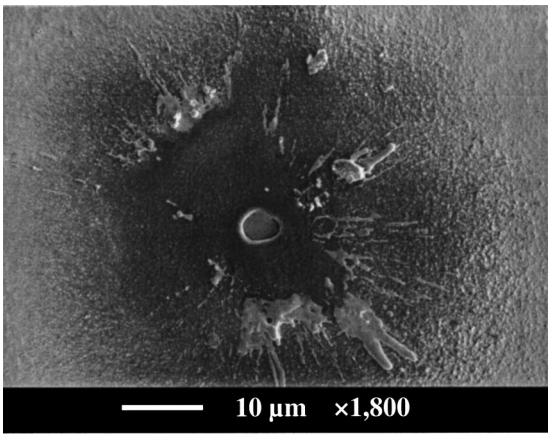

FIG. 11. Scanning electron micrograph of the arc-damaged region from the nitrogen-doped film shown in Fig. 10.

surement. There is a distinct difference in the $I-V$ curves collected before and after the arcing event. Both the shape and signal-to-noise ratio of the $I-V$ curves change significantly after the arc indicating a change in the emission mechanism. As shown in Fig. 10(c), analysis of the $I-V$ data indicate that the threshold field required for emission before and after the arcing event is 250 and 73 V/μm, respectively. Figure 11 shows an SEM micrograph of the arc-damaged region from these measurements. Energy dispersive spectroscopy (EDS) analysis of this region indicate that the irregular material on the surface is molybdenum from the anode.

To ensure that the arcing behavior observed for the nitrogen-doped films was not a characteristic of the field emission system, several undoped carbon films with high sp^2 content were examined. These films were prepared in the same CVD chamber used for the deposition of the nitrogen-doped films grown for this study. The process conditions for these films were as follows: 10% methane in hydrogen, 900 °C substrate temperate, 900 W microwave power, and 20 Torr chamber pressure. The Raman scattering spectra for one of these films is shown in Fig. 12.

These samples were loaded directly into the field emission testing system without any surface pretreatment. Unlike the nitrogen-doped films, these samples exhibited field emission at exceptionally low fields without arcing. Figure 13 illustrates the field emission data taken from one of the measurements. The analysis of the $I-V$ curves taken at several anode-to-cathode distances indicates that the threshold field required for 0.5 nA is ~4 V/μm. This value has been reproduced many times on different areas of the sample surface, as well as among several identically prepared samples. The emission mechanism for these high sp^2 containing carbon films is unclear and is a topic of ongoing research. These field emission results indicate that the arcing behavior, which was observed for nitrogen-doped diamond, is a property of the films, not the field emission apparatus. Possible mechanisms, which produce the microarcing behavior, will be discussed in the next section.

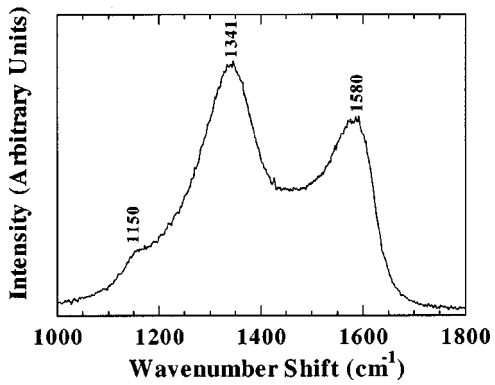

FIG. 12. Raman scattering spectra for an undoped carbon film with high sp^2 content.

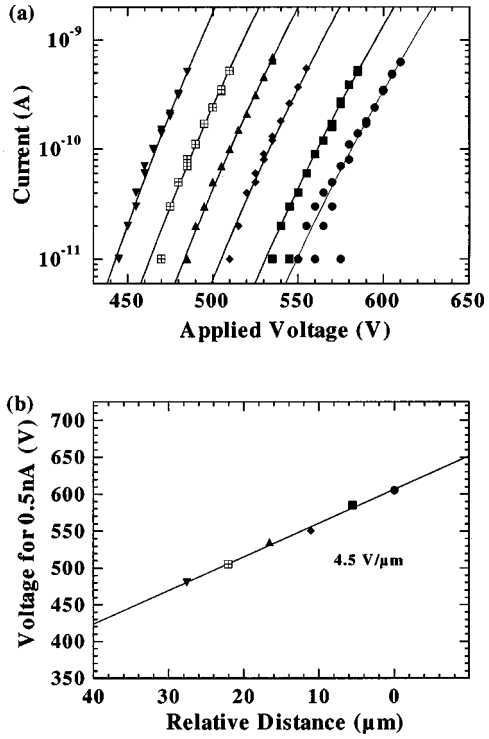

FIG. 13. Field emission measurements of a carbon film with high sp^2 content used to characterize the field emission testing system. Current–voltage measurements are taken at several anode-to-sample distances and are shown in (a). The threshold field vs relative distance for this data set is shown in (b). The threshold field required to obtain 0.5 nA of current are ~4 V/μm.

Ultraviolet photoemission spectroscopy (UPS) is a method of choice for identifying the presence of an NEA for *p*-type diamond surfaces. However, the nitrogen-doped diamond films in this study are highly insulating, which causes charging during UPS analysis. UPS measurements are highly sensitive to charging, which makes this technique unsuitable for the characterization of these nitrogen-doped diamond films.

Photothreshold measurements can also be used to identify an NEA surface. The presence of an NEA for diamond surfaces has been associated with hydrogen termination.[20] This hydrogen termination has been shown to be very stable even after atmospheric exposure. However, hydrogen desorption occurs when diamond films are annealed in excess ~950 °C.[21] These hydrogen free surfaces have been shown to exhibit positive electron affinities (PEA). Thus, observa-

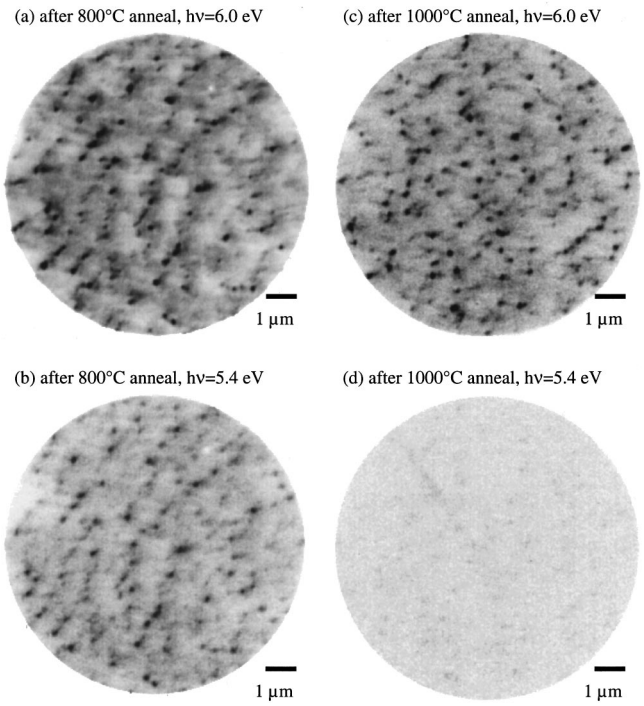

FIG. 14. PEEM images of a hydrogen terminated nitrogen-doped diamond film after 800 and 1000 °C anneals. In these images, the dark regions represent the areas of intense electron emission. Top and bottom images were obtained using 5.4 and 6.0 eV excitation, respectively. The decrease in photoyield for 5.4 eV radiation after the 1000 °C anneal indicates that there is a transition between an NEA and PEA surface.

tion of the photoyield before and after annealing can indicate the presence of a NEA.

Photothreshold measurements of nitrogen-doped diamond films were performed using PEEM along with the tunable spontaneous emission from the Duke University OK-4 ultraviolet free electron laser. In these experiments, nitrogen-doped films were exposed to a remote hydrogen plasma for one minute before being transferred *ex situ* to the PEEM/FEL facility. PEEM images of a nitrogen-doped diamond film taken with 5.4 and 6.0 eV ultraviolet radiation after annealing to 800 and 1000 °C are shown in Fig. 14. For 5.4 eV ($h\nu \approx E_g$) excitation, there is a distinct decrease in the photo yield after annealing to 1000 °C. These results suggest that the original hydrogen terminated surfaces exhibited an NEA. Conversely, for 6.0 eV radiation no apparent change in the photoyield is observed with annealing. This is consistent since for 6.0 eV excitation $h\nu > E_g + \chi$ for either a positive or negative affinity surface.

We attempted to observe emission with all light sources turned off. With the microscope system operated in this mode the image would be due to field emission from the 10 V/μm electric field applied to the surface. This mode is termed field electron emission microscopy (FEEM). No images were detected which is consistent with the high threshold fields observed in the field emission measurements.

IV. DISCUSSION

Using optical emission spectroscopy (OES), several groups have reported the effect of nitrogen addition to H_2–CH_4 plasmas during diamond growth.[22–24] In these studies, nitrogen addition to the plasma produces two additional bands in the emission spectra due to CN radicals and N_2. This is direct evidence that nitrogen can be effectively dissociated by the microwave plasma environment. It has been proposed that species such as CN or HCN can abstract hydrogen from the diamond surface and therefore alter the growth process. Cao *et al.* have suggested that the growth rate increase at low nitrogen concentrations is due to the increased incorporation of these species due to lower desorption rates.[25] At higher nitrogen concentrations, CH species, which have been linked to diamond growth, are reduced in the plasma through the following possible reactions:[23]

$$CH + N \rightarrow H + CN \tag{1}$$

or

$$CH + N_2 \rightarrow HCN + N. \tag{2}$$

The reduction of CH species leads to decreased crystalline quality along with slower growth rates. Ultimately at the highest nitrogen concentrations, no deposition occurs due to the efficient etching of carbon by the CN species. These reports are consistent with the observations of growth rate and crystalline quality of the nitrogen-doped diamond films grown in this study.

Despite the increase of structural defects and nondiamond phases observed in the Raman spectra upon the addition of nitrogen, photoluminescence measurements indicate single substitutional nitrogen incorporation. This means that these films possess the same nitrogen donor level observed in type-Ib HPHT synthetic diamond single crystals. For thin diamond films, the concentration of substitutional nitrogen is difficult to quantify by analytical methods due to the lack of sensitivity for nitrogen, and the tendency for nitrogen to form aggregate defect centers. The nitrogen concentration of homoepitaxial nitrogen-doped diamond films was investigated by Samlenski *et al.* using nuclear reaction analysis.[26] In that study, the nitrogen incorporation for the (100) and (111) growth sectors was $\sim 6.8 \times 10^{17}$ and $\sim 2.3 \times 10^{18}\,\mathrm{cm}^{-3}$, respectively. As a result, the single substitutional nitrogen concentration of the films grown in this study is estimated between 10^{17} and $10^{18}\,\mathrm{cm}^{-3}$. In comparison, the single substitutional nitrogen concentration found in type-Ib HPHT single crystal is $\sim 10^{19}\,\mathrm{cm}^{-3}$.

As stated earlier, field emission from a semiconductor involves (i) the supply of electrons to the semiconductor, (ii) transport of electrons to the surface, and finally (iii) the emission from the surface. In general, field emission measurements will reflect aspects of each of these processes. However, photoemission studies allow the characterization of the emitting surface without being greatly influenced by electron supply or transport. In photoemission measurements, the electrons are photoexcited into the conduction band levels near the surface. By observation of the electrons emitted from the surface, the electron emission properties of the surface can be characterized.

Hydrogen desorption/photothreshold experiments taken with the PEEM/FEL indicate that the nitrogen-doped diamond grown for this study exhibits an NEA when hydrogen

terminated. In addition, the PEEM images show emission from all surfaces with stronger emission from the edges near the surface. The observed enhanced emission from the edges is likely due to field enhancement from the applied field in the microscope. This type of photoemission was observed uniformly across the sample. In contrast, field emission from carbon surfaces has been shown to originate from ''hot spots'' randomly distributed across the film.

In contrast to the nitrogen-doped diamond films prepared by Okano *et al.*, no detectable oxygen or tungsten has been observed for the films examined in this study. In some films PL features attributed to silicon incorporation in diamond have been observed. For comparison, nitrogen-doped films were grown on mirror polished molybdenum substrates. For these films, no silicon related luminescence was observed. However, the field emission properties for the samples grown on either molybdenum or silicon were the same. This suggests that the silicon incorporation observed for some of the films does not appreciably influence the emission mechanism.

Although Geis *et al.* have reported that electrons can be injected into the diamond conduction band through a Schottky barrier, no evidence of this type of emission was observed for the nitrogen-doped diamond films examined in this study. In the Geis model the applied voltage between the anode and cathode drops primarily across the Schottky barrier. Consequently, a very small field is produced between the diamond surface and the anode. Thus, the field emission characteristics are weakly dependent upon the anode-to-cathode distance. In contrast, all field emission measurements in this study exhibited strong linear dependence upon the anode to cathode distance. This dependence suggests that the voltage is dropped across the anode to cathode vacuum gap, rather than the backside contact.

Zhu *et al.* studied the field emission properties of undoped and *p*-type diamond films with varying diamond quality.[17] In that study, there was no clear trend between the content of nondiamond phases in the Raman spectra and the field emission properties. As a result, it was proposed that the presence of graphitic defects alone did not account for the emission characteristics of diamond. On the other hand, a strong correlation between the concentration of structural defects (quantified by the FWHM of the diamond Raman lineshape) and the threshold field required for field emission was observed. Specifically, when the FWHM of the diamond peak was greater than 7–11 cm^{-1} the threshold fields were typically less than 50 V/μm. It was suggested that the diamond defects create additional energy bands within the band gap of diamond and thus contribute electrons for emission at low fields. In contrast to that work, the field emission characteristics of the nitrogen-doped films in these experiments do not correlate with the FWHM of the diamond Raman peak.

By studying the interaction of the nitrogen donors and the defects present in the films, the discrepancies between our field emission results and the reports of Zhu and Geis may be explained. In 1991, Mort *et al.* measured the electrical conductivity of undoped and nitrogen-doped films deposited by hot filament CVD.[27] In that study, electrical measurements of undoped diamond films indicated the conductivity was due to transport through in-gap defect states. Furthermore, it was established that these states were identified as acceptors. For nitrogen-doped films, it was observed that the electrical conductivity was less than that for undoped diamond films by a factor of 10^3 at room temperature and 10^6 at 400 K. This effect was attributed to the compensation of the defect acceptor states by nitrogen donors.

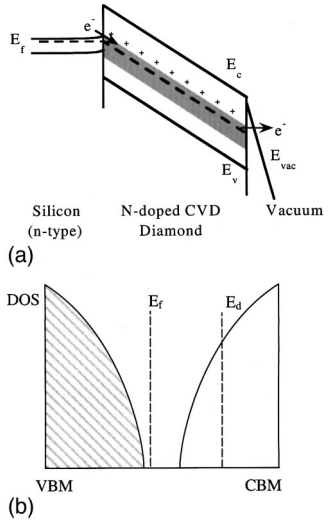

FIG. 15. (a) A schematic energy band diagram illustrating the defect enhanced field emission model from compensated nitrogen-doped diamond. The density of in-gap states is illustrated in (b). The shaded regions correspond to filled states. The nitrogen donors are compensated by the distribution of in-gap defect states. As a result, the resistance of the film increases as the defect band approaches a completely filled band.

The effects of compensation have implications upon the Geis emission model. If the nitrogen-doped diamond is compensated, then the formation of a Schottky depletion layer will be inhibited and electron injection into the conduction band will not occur. This is consistent with the field emission results presented in this study. In addition, we observed no dependence of the field emission properties upon the nucleation method or substrate. This suggests that the field emission mechanism is limited more by the bulk diamond film than the supply of electrons to the film.

We suggest that the defect enhanced field emission model proposed by Zhu *et al.* can be extended to include compensation effects observed in this study. At low nitrogen concentrations, the in-gap defect states are compensated by the nitrogen donors. Therefore, the density of defect states available for ''hopping'' conduction is reduced thus greatly increasing the threshold field required for electron emission. As the nitrogen concentration in the process gas is increased, more defects in the film are created. It is assumed that despite the increase in the nitrogen gas concentration, the amount of nitrogen incorporated in the diamond film remains relatively constant. Eventually at the highest nitrogen concentrations, there are enough in-gap defect states present in the material to overcome the effects of nitrogen compensation. As a result, defect enhanced electron field emission begins to occur. This emission mechanism is illustrated in Fig. 15.

As mentioned previously, field emission is often preceded by microarcing for nitrogen-doped diamond. This behavior is similar to that reported by Gröning *et al.*[19] In that study, it was reported that the localized pressure between anode and cathode increases due to electron stimulated desorption from electrons striking the anode.[19] Ultimately, a discharge occurs creating craters on the diamond surface. This model suggests that arcing would be a property of the anode material not the cathode. However, our experiments have indicated that field emission can be obtained from carbon films with high sp^2 content without arcing. In addition with pressures less than 10^{-8} Torr, one would expect that eventually all adsorbed species on the anode would be removed and the arcing behavior would cease. Our experiments have not indicated a decrease in arcing with time.

As a result of these observations, we suggest that the increase in local pressure is due to properties of the cathode, not the anode. Field emission studies from diamond have indicated that electrons are emitted from random emission sites across the sample. This ''spotty'' emission coupled with the highly insulating nature of the nitrogen-doped films can produce large resistive heating on a microscopic scale. We suggest that this heating causes trapped gases (e.g., hydrogen, nitrogen etc.) in the diamond film to be released causing vacuum breakdown within the gap. In this study, samples with the highest nitrogen process gas concentrations exhibit higher conductivity and are less susceptible to arcing. For a future research goal, it may be possible to distinguish the source of the plasma using a residual gas analyzer during the field emission measurements.

V. CONCLUSION

The objective of this work was to grow high quality nitrogen-doped diamond films and to determine the role of nitrogen in these films. However, the diamond film quality is diminished by even small nitrogen concentrations in the process gas. The field emission properties of films with [N]/[C] gas phase concentrations up to 48 have been measured. Despite evidence of single substitutional nitrogen doping, detectable field emission in most cases is preceded by an arcing event that causes damage to the film and substrate and significantly changes the emission properties. Analysis of $I-V$ data from the films that exhibit electron emission prior to arcing indicate that extremely high fields (100–300 V/μm) are required for field emission. It is likely that the required threshold fields for the samples that exhibit arcing before emission exceed 300 V/μm.

We suggest that the nitrogen donors incorporated into these diamond films are compensated by in-gap defect states. By considering compensation effects, the apparent contradiction between the defect enhanced field emission model proposed by Zhu *et al.* and the field emission characteristics of the nitrogen-doped diamond films in this study can be explained. This compensation reduces the density of in-gap states and increases the threshold field required for electron emission. It is evident that these compensation effects need to be controlled in order to investigate the properties of nitrogen in CVD diamond films.

ACKNOWLEDGMENTS

The authors would like to thank the Duke University Free Electron Laboratory for access to the OK-4 UV FEL. We gratefully acknowledge the financial support of the Office of Naval Research, the Japan Fine Ceramics Center, and Kobe Steel USA. We would like to express our appreciation to Dr. David L. Dreifus, Dr. Linda S. Plano, and Dr. Brian R. Stoner for their participation in many interesting discussions and their invaluable suggestions.

[1] F. J. Himpsel, J. A. Knapp, J. A. van Vechten, and D. E. Eastman, Phys. Rev. B **20**, 624 (1979).
[2] B. B. Pate, Surf. Sci. **120**, 83 (1986).
[3] J. van der Weide, Z. Zhang, P. K. Baumann, M. G. Wensell, J. Bernholc, and R. J. Nemanich, Phys. Rev. B **50**, 5803 (1994).
[4] J. van der Weide and R. J. Nemanich, J. Vac. Sci. Technol. B **12**, 2475 (1994).
[5] P. K. Baumann and R. J. Nemanich, J. Appl. Phys. **83**, 2072 (1998).
[6] R. G. Farrer, Solid State Commun. **7**, 685 (1969).
[7] R. G. Farrer and L. A. Vermeulen, J. Phys. C **5**, 2762 (1972).
[8] M. W. Geis, J. C. Twichell, J. Macaulay, and K. Okano, Appl. Phys. Lett. **67**, 1328 (1995).
[9] M. W. Geis, N. N. Efremow, K. E. Krohn, J. C. Twichell, T. M. Lyszczarz, R. Kalish, J. A. Greer, and M. D. Tabat, Lincoln Lab. J. **10**, 3 (1997).
[10] K. Okano, S. Koizumi, S. R. P. Silva, and G. A. J. Amaratunga, Nature (London) **381**, 140 (1996).
[11] R. Matsuda, K. Okano, and B. B. Pate, Mater. Res. Soc. Symp. Proc. **509**, 59 (1998).
[12] B. R. Stoner, B. E. Williams, S. D. Wolter, K. Nishimura, and J. T. Glass, J. Mater. Res. **7**, 257 (1992).
[13] C. H. Wu, W. H. Weber, T. J. Potter, and M. A. Tamor, J. Appl. Phys. **73**, 2977 (1993).
[14] J. van der Weide and R. J. Nemanich, Phys. Rev. B **49**, 13629 (1994).
[15] E. Bauer, Inst. Phys. Conf. Ser. **119**, 1 (1991).
[16] L. H. Veneklasen, Rev. Sci. Instrum. **63**, 5513 (1992).
[17] W. Zhu, G. P. Kochanski, S. Jin, L. Seibles, D. C. Jacobson, M. McCormack, and A. E. White, Appl. Phys. Lett. **67**, 1157 (1995).
[18] L. Bergman, M. T. McClure, J. T. Glass, and R. J. Nemanich, J. Appl. Phys. **76**, 3020 (1994).
[19] O. Gröning, O. M. Küttel, E. Schaller, P. Gröning, and L. Schlapbach, Appl. Phys. Lett. **69**, 476 (1996).
[20] J. van der Weide and R. J. Nemanich, Appl. Phys. Lett. **62**, 1878 (1993).
[21] P. K. Baumann and R. J. Nemanich, Surf. Sci. **409**, 320 (1998).
[22] R. Locher, C. Wild, N. Herres, D. Behr, and P. Koidl, Appl. Phys. Lett. **65**, 34 (1994).
[23] T. Vandevelde, M. Nesladek, C. Quaeyhaegens, and L. Stals, Thin Solid Films **290/291**, 143 (1996).
[24] H. Chatei, J. Bougdira, M. Rémy, P. Alnot, C. Bruch, and J. Krüger, Diamond Relat. Mater. **6**, 107 (1997).
[25] G. Cao, J. Schermer, W. van Enckevort, W. Elst, and L. Giling, J. Appl. Phys. **79**, 1357 (1996).
[26] R. Samlenski, C. Haug, R. Brenn, C. Wild, R. Locher, and P. Koidl, Appl. Phys. Lett. **67**, 2798 (1995).
[27] J. Mort, A. Machonkin, and K. Okumura, Appl. Phys. Lett. **59**, 3148 (1991).